

Adsorption of the Butene Isomers in Faujasite: A Combined *ab-Initio* Theoretical and Experimental Study

Frederik Tielens,[†] Joeri F. M. Denayer,[‡] Inge Daems,[‡] Gino V. Baron,[‡]
Wilfried J. Mortier,[§] and Paul Geerlings^{*,†}

Eenheid Algemene Chemie (ALGC), Fakulteit Wetenschappen, Vrije Universiteit Brussel, Pleinlaan 2, B-1050 Brussels, Belgium, Dienst Chemische Ingenieurstechnieken (CHIS), Fakulteit Toegepaste Wetenschappen, Vrije Universiteit Brussel, Pleinlaan 2, B-1050 Brussels, Belgium, and European Technology Center, ExxonMobil Chemical Europe Inc., Hermeslaan 2, B-1831 Machelen, Belgium

Received: November 7, 2002; In Final Form: April 2, 2003

The adsorption behavior of the butene isomers on NaY zeolite is studied experimentally and compared with quantum chemical predictions. The adsorption experiments were carried out with the pulse chromatographic method, the calculations were performed both on the HF as on the DFT-B3LYP level in combination with the 6-31G* and the 6-311+G** basis set. The results of the calculations are in line with the experimental ones for the cation–butene isomer interaction in the gas phase; the same adsorption trend in the zeolite cluster, however, could not be recovered. The calculated interaction energies for a Na⁺ zeolite cluster are close to the experimental ones with a magnitude of deviation of only 2 kcal/mol, showing the reliability of the model chosen. The trends obtained are discussed in the framework of the HSAB principle and purely electrostatic and inductive interactions.

Introduction

The use of α -olefins has found many industrial applications; besides polymer chemistry in general, long chain olefins are used for the production of detergents, while short chain olefins are used in, for example, alkylation reactions for the production of multi-branched alkanes with high octane numbers. Therefore the separation of α -olefins and inter-olefins is of considerable economic importance. In the case that they are used as monomers, one needs high purity α -olefin feedstocks or enriched linear α -olefin (LAO) streams, e.g. obtained by distillation. Nevertheless, many valuable compounds are lost in the gasoline pool.

The separation of α -olefins is very complex and is performed on an industrial level through extractive distillation and several reactions: the most difficult being the separation of 1- and 2-butene. For this separation one uses an adsorption procedure on molecular sieves, namely the UOP “sorbutene” process.¹ Very little information is available with respect to this process. Some molecular dynamics studies were performed to study adsorption and diffusion properties of butenes^{2–4} in zeolites.

The molecular sieves that are of interest in this application are zeolites. Zeolites are of widespread use in industrial catalytic and adsorption processes and have been used since the 1950s. Today it is possible to synthesize very pure and perfect crystals, which are highly suited as reference for theoretical studies such as the present one.^{5,6}

Zeolites are three-dimensional aluminosilicates containing cages and channels of molecular dimension acting as micro-reactors. The presence of exchangeable cations in the lattice makes them even more selective for specific interactions. The

concentration and position, i.e., distribution of the cations depend on the structure as well as on the silicon/aluminum ratio of the lattice, which also can be predicted through theoretical calculations.⁷ Each tetrahedral aluminum introduces a net negative charge, which has to be compensated by the cation.

For the design and control of adsorptive separation processes, a good knowledge of the adsorption properties is a prerequisite. To develop a new adsorbent for the separation of a specific group of molecules, a broad experimental study has to be performed by a trial and error procedure. A more rational design would invoke the use of modern computational techniques, such as present day quantum chemical *ab initio* calculations.

The *ab initio* study of adsorption properties is still computationally demanding, but with the ever increasing computing power these “theoretical experiments” will become more accessible. In the past, our group has already studied very intensively the adsorption properties of small molecules in zeolite-type adsorbents on an *ab-initio* level.^{8–13} Full *ab-initio*, non-empirical calculation strategies were presented for the prediction of Henry constants, heats of adsorption, separation constants, and adsorption energy surfaces.¹³ On the other hand, other groups presented the first quantum chemically calculated isotherm.¹⁴

In this paper, the very first fully *ab-initio* optimized geometries and *ab-initio* interaction energies of the butene isomers (1-butene, *cis*-2-butene, *trans*-2-butene, and iso-butene) in NaY zeolites are studied and compared with the experimental heats of adsorption. Experimentally, new measurements are presented based on the pulse chromatographic method^{16,17} and compared to the measurements of Harfinger obtained via the gravimetric method.

The experimental results are interpreted within the framework of conceptual DFT using the Hard and Soft Acids and Bases (HSAB) principle of Pearson,¹⁵ in which various groups have been active during the past decade (for reviews see refs 18–23).

* Author to whom correspondence should be addressed. Tel.: +32.2.629.33.14. Fax: +32.2.629.33.17. E-mail: pgeerlin@vub.ac.be.

[†] Eenheid Algemene Chemie (ALGC), Fakulteit Wetenschappen, Vrije Universiteit Brussel.

[‡] Dienst Chemische Ingenieurstechnieken (CHIS), Fakulteit Toegepaste Wetenschappen, Vrije Universiteit Brussel.

[§] European Technology Center, ExxonMobil Chemical Europe Inc.

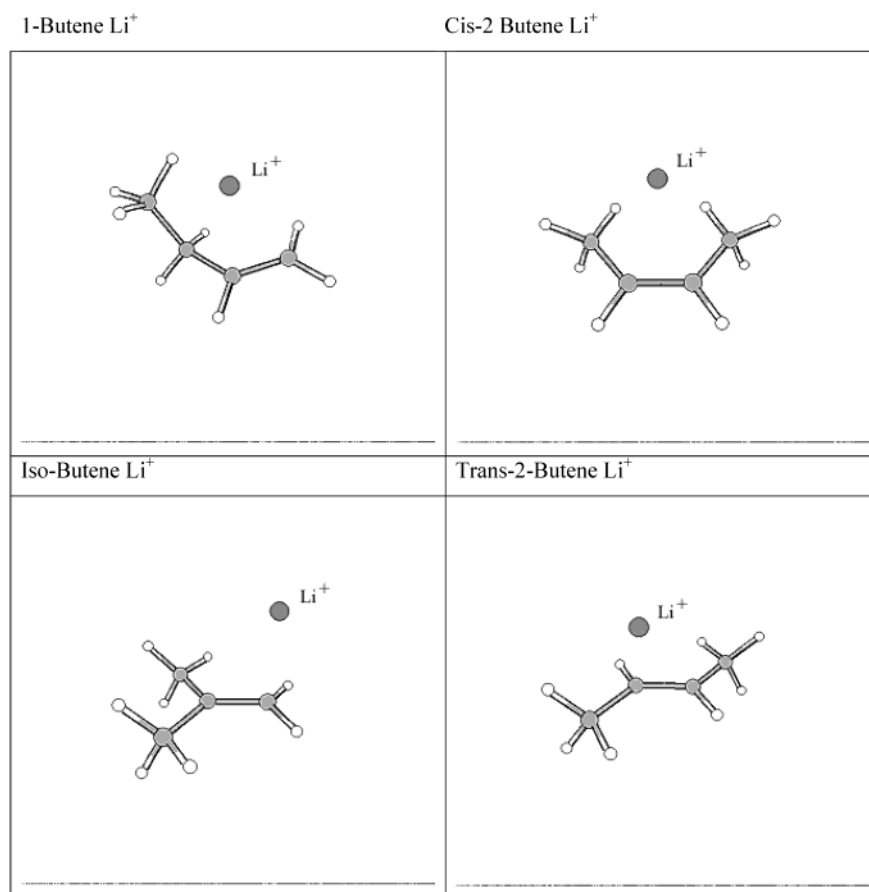


Figure 1. Butene isomers in interaction with a cation (Li⁺).

Experimental Details

Adsorption enthalpies of isobutene, 1-butene, *cis*-butene, *trans*-butene, and butane were determined by the chromatographic method.²¹ The experiments were performed with a NaY zeolite (kindly provided by EXXONMOBIL). This zeolite has a Si/Al ratio equal to 3.8 and unit cell vertexes equal to 245.7 pm.^{5,6}

The zeolite powder was compacted into solid disks by applying a pressure of about 300 bar, and broken subsequently into fragments. The fraction from 250 to 400 μm was filled into a 1/8-in. diameter stainless steel column with a length of 0.19 m.

Activation of the adsorbent was performed under continuous He flow by raising the temperature at a rate of 5 °C/min to 400 °C and maintaining this temperature overnight. The hydrocarbon gases were of analytical grade and purchased from l'Air Liquide.

Henry constants were determined using the tracer chromatographic technique.²⁴ In this technique, the compound of interest is injected in an inert carrier gas flowing through the column packed with adsorbent. The first moment of the response curve of the injected component and its Henry constant K' are correlated as follows:

$$\mu = \frac{L}{v_f} [(\epsilon_{\text{ext}} + \epsilon_{\text{macr}}) + (1 - \epsilon_{\text{ext}} - \epsilon_{\text{macr}})RT\rho_c K'] \quad (1)$$

where L is the column length, v_f the superficial velocity in adsorbent column, ϵ_{ext} the external porosity, ϵ_{macr} the macro porosity, and ρ_c the crystal density.

The measurements were performed in the temperature range from 160 to 220 °C, with temperature intervals of 15 °C, and using helium as carrier gas.

The enthalpy ΔH_0^θ and entropy $\Delta S_{0,\text{local}}^\theta$ of adsorption at low coverage were calculated from the temperature dependence of the Henry constants (eq 2):

$$\ln(K'_0) = \frac{-\Delta H_0^\theta}{RT_m} + \left[\frac{\Delta S_{0,\text{local}}^\theta}{R} + \ln\left(\frac{n_T}{2p^\theta}\right) \right] \quad (2)$$

The subscript 0 refers the zero coverage limit, T_m is the average experimental temperature and p^θ refers to the standard state of the gas phase (chosen as 1 atm). n_T equals the number of adsorption sites, and is equal to the number of cations present in the zeolite framework.²⁴

With respect to the adsorption entropy, two extreme models can be considered: a nonlocalized model, in which molecules retain 2-dimensional translational freedom on the adsorption surface, and a localized model, in which molecules are adsorbed on well-defined adsorption sites. In the first model, molecules loose 1 degree of translational freedom, while all degrees of translational freedom are lost in the second model on transition from the gas phase to the adsorbed state. It has already been demonstrated several times that the adsorption of alkanes and alkenes on zeolites occurs preferentially on the Brønsted acid sites or the compensation cations of the zeolite, corresponding to the localized adsorption model.^{25,26} Moreover, the latter model represents the closest the model in the ab initio calculations. Equation 2 was developed for the localized adsorption model.^{27–30}

Computational Details

Since the major adsorption sites in the zeolite cavity are the cations, an introductory study is made by approximating the

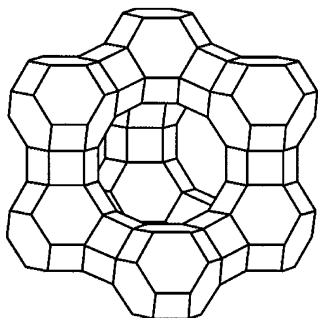


Figure 2. Framework structure of faujasite.

adsorption site by a single cation. This allows us to determine the afterward influence of the zeolite cage in the adsorption process.

As mentioned above, four isomers of butene were investigated: isobutene, 1-butene, *cis*-2-butene, and *trans*-2-butene (see Figure 1). These butenes were optimized with and without interacting cation in order to obtain the corresponding interaction energies. Six different cations were considered: Li^+ , Na^+ , K^+ , Be^{2+} , Mg^{2+} , and Ca^{2+} .

Adsorption geometries in the gas phase were obtained for all 24 combinations (cation/isomer) using a DFT approach with the B3LYP functional,^{31,32} which has proven its reliability,^{33,34} in combination with the 6-31G* and 6-311+G** bases.³⁵ These calculations were carried out with the Gaussian98 program³⁶ running on a Compaq Digital DS20 workstation. Conventional Hartree–Fock (HF) results with the same basis are given for comparison and completeness; they were performed with the BRABO program.³⁷

In the second part, the zeolite cluster was taken into account, and adsorption geometries were calculated for the isomers in the NaY zeolite, using the Gaussian98 program. The adsorption complex, i.e., the hydrocarbon together with the zeolite cluster, was treated on the B3LYP/6-31G* level.

The zeolite clusters used in our calculations are based on the large α -cages of the high alumina faujasite NaY (see Figure 2). The extraframework cations present in NaY are site I and site II Na^+ , no other type of cation is present. This makes the zeolite crystal structure easier to model, in most other zeolites the cations are distributed over a range of possible sites.

Due to time and computational power limitations, we were forced to set up a calculation model on the basis of the following assumptions and approximations:

A. To prevent any under- or over-estimation of the interaction energies due to a non zero charge, the cluster was made electrically neutral by adding two cations, resulting in a Si/Al ratio of 5 (see Figure 3), in comparison with the experimental value of 3.8. For symmetry reasons a cluster corresponding to 1/4 of a cavity (8 cavities/unit cell) terminated with OH-groups was used. This cluster contained 65 atoms, its formula being $\text{Si}_{10}\text{Al}_2\text{Na}_2\text{O}_{33}\text{H}_{18}$ (see Figure 3).

B. The zeolite cluster (aluminosilicate framework + cation) was kept fixed during the calculation (full optimization of the butene isomer). The effect of the framework relaxation is expected to be negligible due to the relative small size of the butene molecule and its nonpolar character.

C. Although the size of the cluster used was large for the type of calculations performed in this work, one should acknowledge its limitations. Theoretically, the influence of the cluster size on the adsorption energies can be calculated, but this type of calculation is beyond the scope of this study.³⁸

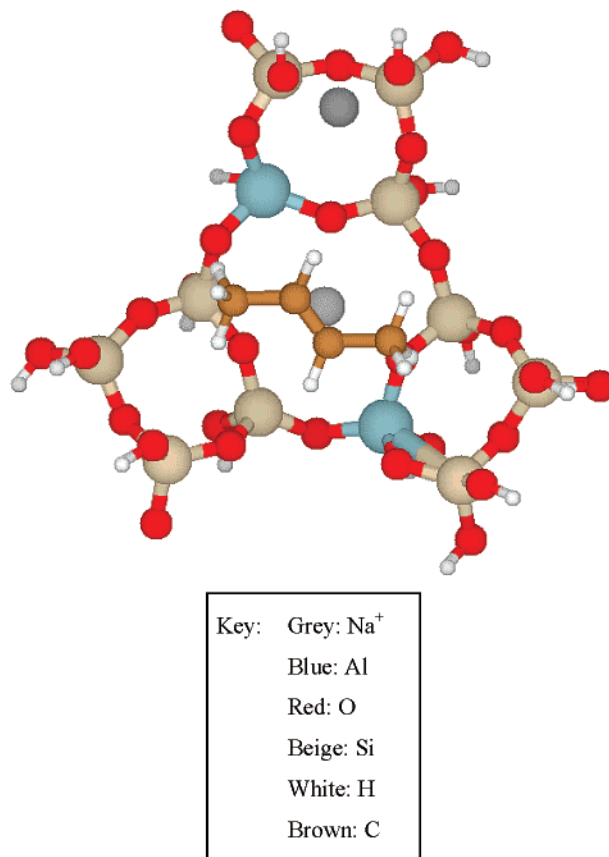


Figure 3. *trans*-2-Butene in interaction with site II of NaY.

D. The basis set superposition error (BSSE) corrections were not considered in view of high computational costs (price/quality). However, in view of the relatively large basis sets, the effect can be expected to be small, certainly when considering trends.³⁹

E. The present quantum chemical calculations were performed at 0 K, and neglect the possibility to “jump” from one conformation or adsorption site to another. Experimental results were obtained at higher temperatures, where the potential energy well becomes a more spread area. Taking this effect into account in our static approach is impossible at the level of computation considered (hitherto, inclusion of entropic effects has unavoidably been performed at a much lower computational level⁴⁰).

F. Although electron correlation is included at a relatively good level (B3LYP), dispersion forces are not accounted for in the model, because the zeolite is highly ionic and we expect these forces to be relatively small in comparison with the electrostatic forces generated by the presence of the cations (covering also induction energies).

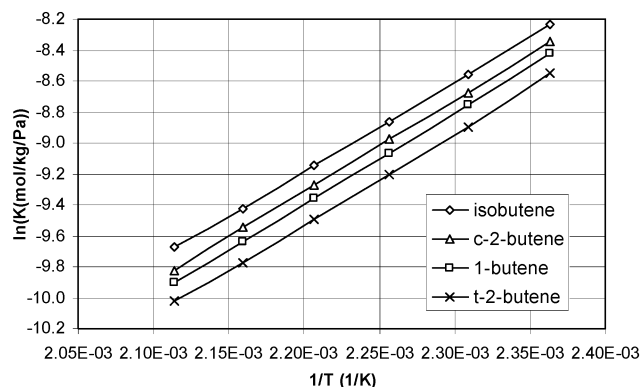
One of the aims of this investigation is the calculation of adsorption enthalpies ΔH_0^θ . Since all cavities are considered identical, only one cavity was modeled. The experimental adsorption enthalpy ΔH_0^θ can be approximated by the average interaction energy $\overline{\Delta E}$ over the different possible minima in the cavity, as follows:

$$\Delta H_0^\theta \approx \overline{\Delta E} \quad (3)$$

The value of $\overline{\Delta E}$ in this equation should be considered as the average value of ΔE , calculated by integration over all positions and orientations of the adsorbing molecule, weighted according to a Boltzmann factor.

TABLE 1: Experimental Henry Constants, Adsorption Enthalpies, and Adsorption Entropies of the Butene Isomers on Na–Y

| | K' (mol/kg/Pa) 170 °C | ΔH_0^θ (kJ/mol) | ΔS_0^θ (J/molK) | ΔH_0^θ (kJ/mol) ^a |
|------------------------|-------------------------------|---------------------------------|---------------------------------|--|
| isobutene | 1.41×10^{-4} | -49.0 ± 0.6 | -80.0 | |
| 1-butene | 1.15×10^{-4} | -48.9 ± 0.3 | -81.2 | -60.5 |
| <i>cis</i> -2-butene | 1.26×10^{-4} | -49.0 ± 0.2 | -80.9 | -60.8 |
| <i>trans</i> -2-butene | 1.01×10^{-4} | -48.7 ± 0.4 | -81.9 | -59.0 |
| <i>n</i> -butane | 3.19×10^{-5} | -37.1 ± 0.1 | -67.3 | -51.5 |

^a Ref 16.**Figure 4.** Experimental van't Hoff plots of butene isomers on NaY.

$$\overline{\Delta E} = \sum_i x_i \Delta E_i \quad (4)$$

with

$$x_i = e^{-\Delta E_i/RT} \quad (5)$$

Combining eqs 3, 4, and 5, one obtains:

$$\Delta H_0^\theta \approx \overline{\Delta E} \approx \Delta E_{\min} \quad (6)$$

indicating that the corresponding interaction energy, found after an ab-initio optimization, is (in first approximation) equal to the heat of adsorption. Except at high temperatures one could expect the molecules to be mostly located close to the deepest potential minimum.²⁴

Results

Experimental Results. Figure 2 shows the experimental van't Hoff plots of the butene isomers. The low coverage adsorption enthalpies and entropies, obtained by linear regression of the experimental data using eq 2, are given in Table 1. For comparison, the adsorption enthalpy of butane is also given in this table.

Experimentally one finds that isobutene has the highest Henry constant at all experimental temperatures (Figure 4), followed in order by *cis*-2-butene, 1-butene, and finally *trans*-2-butene. At 170 °C, the difference in Henry constant between the 2 extremes (isobutene and *trans*-2-butene) is about 40% (see Table 1). Adsorption isotherms measured using a gravimetric technique by Harlfinger et al.¹⁶ on a NaX zeolite with a Si/Al ratio of 1.8 also show a decrease in amounts adsorbed in the order: *cis*-2-butene, 1-butene and finally *trans*-2-butene (see Table 1).

The differences in experimental adsorption enthalpies at zero coverage between the butene isomers are small and lie within the margin of experimental error, which is relatively small and

TABLE 2: HF Interaction Energies ΔE of the Butene Isomers with Different Types of Cations (in kJ/mol)

| | | isobutene | 1-butene | <i>cis</i> - 2-butene | <i>trans</i> - 2-butene |
|------------------|--------|-----------|----------|--------------------------|----------------------------|
| Li ⁺ | 6-31G* | -107.92 | -99.86 | -100.23 | -98.32 |
| Na ⁺ | 6-31G* | -78.73 | -76.64 | -75.25 | -73.44 |
| K ⁺ | 6-31G* | -53.59 | -53.93 | -54.05 | -50.70 |
| Be ²⁺ | 6-31G* | -795.36 | -806.83 | -801.40 | -729.00 |
| Mg ²⁺ | 6-31G* | -423.82 | -385.50 | -384.19 | -378.96 |
| Ca ²⁺ | 6-31G* | -212.83 | -203.02 | -193.35 | -192.73 |

TABLE 3: DFT-B3LYP Interaction Energies ΔE of the Butene Isomers with Different Types of Cations (in kJ/mol)

| | | isobutene | 1-butene | <i>cis</i> - 2-butene | <i>trans</i> - 2-butene |
|------------------|-----------|-----------|----------|--------------------------|----------------------------|
| Li ⁺ | 6-31G* | -128.72 | -128.71 | -124.14 | -123.49 |
| | 6-311+G** | -117.21 | -115.79 | -114.48 | -113.61 |
| Na ⁺ | 6-31G* | -90.19 | -90.00 | -87.81 | -85.96 |
| | 6-311+G** | -78.81 | -76.14 | -76.48 | -74.48 |
| K ⁺ | 6-31G* | -53.68 | -53.70 | -52.06 | -51.03 |
| | 6-311+G** | -47.27 | -44.36 | -45.75 | -44.95 |
| Be ²⁺ | 6-31G* | -832.12 | -884.91 | -984.99 | -827.30 |
| | 6-311+G** | -817.92 | -866.14 | -974.94 | -814.34 |
| Mg ²⁺ | 6-31G* | -474.24 | -459.11 | -426.24 | -435.40 |
| | 6-311+G** | -456.56 | -441.48 | -410.72 | -418.52 |
| Ca ²⁺ | 6-31G* | -243.26 | -239.84 | -231.25 | -227.36 |
| | 6-311+G** | -262.46 | -255.31 | -261.05 | -255.03 |

amounts to only a few tenths of a kJ/mol. The adsorption enthalpies obtained by Harlfinger et al.,¹⁶ given in Table 1, show the same tendency, although the absolute values are higher (about 10 kJ/mol) than the ones obtained in this work. This difference can be attributed to the use of a different zeolite with a higher Al content (NaX, Si/Al 1.8 compared to a Si/Al of 3.8 for the studied zeolite). Harlfinger's measurements were performed with a different experimental technique at a minimum loading of 1 molecule/supercage, while our measurements were done at much lower zeolite loadings.

Theoretical Results. In the first part the molecules were optimized in the gas phase. Two methods were used, the HF and B3LYP method in combination with the 6-31G* and 6-311+G** basis sets. This was followed by the calculation of the interaction of the butene isomers with a series of cations (Li⁺, Na⁺, K⁺, Be²⁺, Mg²⁺, Ca²⁺) (see Table 2). From the HF results, one can observe a better interaction for isobutene with a cation in the gas phase in comparison with the other considered isomers. Only for K⁺ and Be²⁺, the interaction with isobutene is less important. The latter can thus be related to the calculation level and/or to the radius/charge ratio of the cation.

Among the four isomers, *trans*-2-butene has the lowest affinity to bind with a cation, which is in agreement with the experiment of Harlfinger et al.¹⁶ done with a NaX zeolite (Si/Al = 1.8) and also with our experimental results (see Table 1). Between 1-butene and *cis*-2-butene, the smallest differences are found.

Looking at the DFT results from Table 3, we find roughly the same trend as for the HF results, though the results can be expected to be more reliable for the absolute values and of course the interaction trends.

The interaction energy differences between 1-butene and *cis*-2-butene increase, even change sign, with decreasing radius (Li⁺: 59 pm, Na⁺: 102 pm, K⁺: 138 pm, Be²⁺: 27 pm, Mg²⁺: 72 pm, Ca²⁺: 100 pm),⁴¹ and increasing charge of the cation, (-1.31 kJ/mol, 0.34 kJ/mol, 1.39 kJ/mol, and -118.20 kJ/mol, -30.76 kJ/mol, 5.74 kJ/mol for the alkali and alkaline earth cations, respectively).

TABLE 4: Interaction Energies (B3LYP/6-31G*) of the Butene Isomers with the Na⁺ Zeolite Cluster (ΔE in kJ/mol)

| | ΔE |
|------------------------|------------|
| isobutene | -54.43 |
| 1-butene | -66.11 |
| <i>cis</i> -2-butene | -58.94 |
| <i>trans</i> -2-butene | -50.91 |

The geometries calculated at the highest calculation level for the interaction with Li⁺ (B3LYP/6-311+G**) are shown in Figure 1.

Comparison of the results with the largest and thus the most reliable basis set between the cations leads to the following conclusions: from the three isomers 1-butene, *cis*-2-butene, and *trans*-2-butene, *cis*-2-butene adsorbs the best when a cation with a large radius and a low charge is involved, for a small cation with a high charge 1-butene becomes better.

We will now try to interpret adsorption trends both in terms of properties of the zeolite framework and the electrical properties (dipole moment, polarizability, and softness) of the gases. This study was performed by modeling the NaY zeolite (see Figure 3) as is described in the computational details, yielding a cluster of 65 atoms.

In Table 4 we present the interaction energies after optimization of the geometry for each isomer in interaction with the Na-zeolite cluster mimicking the site II adsorption site (site II is the only site available for adsorption (vide infra)). A first and overall statement is that the theoretical values are very close to the experimental ones: indeed, the difference between theory and experiment is only of the order of 10 kJ/mol, i.e., 2.5 kcal/mol, which is close to the "chemical accuracy" of 1 kcal/mol aimed at by quantum chemists.

It should be emphasized that the interaction energy differences are small (all energies are situated in a range of 15.2 kJ/mol, i.e., 3.63 kcal/mol), (cf. quantum chemical accuracy of approximately 1 kcal/mol). Experimentally even smaller differences are found between the adsorption enthalpies of the different isomers, a few tenths of a kJ/mol! The relative ordering of the results on the other hand can be explained as follows.

From the results of Table 4, one observes a shift in the theoretically obtained adsorption trend compared to the calculations with isolated cations in the gas phase. 1-Butene now shows a more favorable adsorption enthalpy than isobutene. *Trans*-2-butene has still the lowest affinity to interact with the cation/zeolite in comparison with the other isomers.

This trend can still be explained on the basis of the radius/charge ratio of the exchangeable cation in the zeolite. Due to charge transfer to the zeolite framework, the cation reduces in size. The charge of the cation itself can deplete up to 40% of its initial charge. So, from the results obtained for the single cation interaction, it is known that a smaller cation is better suited to interact with 1-butene than with *cis*-2-butene (see Tables 2 and 3), e.g., Li⁺/1-butene: -115.79 kJ/mol versus Li⁺/*cis*-2-butene: -114.48 kJ/mol and K⁺/1-butene: -44.36 kJ/mol versus K⁺/*cis*-2-butene: -45.75 kJ/mol.

The interaction behavior of molecules is dependent on different factors and can be interpreted both in terms of traditional theory of intermolecular interactions, involving permanent and induced electrical moments or factors determining them (μ , α , ...) ⁴² and in terms of the HSAB principle, ¹⁵ which was used by our group to predict/investigate several molecular interactions. ¹⁹⁻²¹ To understand better the theoretically obtained adsorption trend, the interaction energies are confronted with two electrical properties of the molecules, namely, the polarizability and the dipole moment, calculated at

TABLE 5: Dipole Moments, μ , Polarizabilities, α , and Global Softness S of the Butene Isomers with the Zeolite Cluster, (μ , α , and S in au) Calculated on the B3LYP/6-311+G Level, and Experimental Data**

| | μ | α | α_{expt}^a | S |
|------------------------|-------|----------|--------------------------|------|
| isobutene | 0.230 | 50.47 | 55.97 | 3.94 |
| 1-butene | 0.163 | 50.71 | 57.52 | 3.85 |
| <i>cis</i> -2-butene | 0.100 | 50.37 | 57.32 | 4.06 |
| <i>trans</i> -2-butene | 0.000 | 50.95 | 57.32 | 3.89 |
| <i>n</i> -butane | 0.000 | 50.65 | 55.35 | 2.99 |

^a Ref 43.

the B3LYP/6-311+G** level (see Table 5) and the global softness S , ⁴⁴ also calculated at the same level using the following approximation:

$$S = \frac{1}{\epsilon_{\text{LUMO}} - \epsilon_{\text{HOMO}}} \quad (7)$$

where ϵ_{HOMO} and ϵ_{LUMO} are the orbital energies of the highest occupied and unoccupied orbitals, respectively. The results for the softness are also very similar, as was found for polarizabilities and the interaction energies. This confirms the likeness of the butenes and the difficulty in separating them.

It is clear that the single nonpolar molecule (*trans*-2-butene) yields the lowest interaction energy, as can be seen in the majority of our calculations. This is due to fact that in the cavity of a cationic zeolite one deals with a strong internal electric field, in which the first-order effects due to permanent multipole moments are dominating and in which the second-order effects are difficult to judge. As *trans*-2-butene, *n*-butane does not have a dipole moment and the lowest polarizability of both, showing, as expected, the poorest adsorption affinity to the zeolite. For the other molecules there is not such a clear-cut trend with the dipole moment; however, when both electrical properties are combined (dipole moment and polarizability), the obtained trend becomes more obvious. When the dipole moments are of the same order of magnitude, the polarizability plays the dominating role and certainly when there is no dipole moment at all. In that case, the polarizability dominates and the Softness values are in line with the interaction trend (see *Trans*-2-butene and *n*-butane). Looking to the global softness, 1-butene has the lowest softness S , i.e., the highest hardness, of the butene isomers, which, applying the HSAB principle, would interact preferably with the hard Na-cation ($S = 0.849$ au; B3LYP/6-311+G**), as is predicted in our cluster calculation.

As a whole the results are in line with the chemical intuition that the interaction of nonpolar molecules with a zeolite is strongly enhanced upon the presence of a strong electrostatic field in the zeolite favoring larger induction energies.

Discussion

The theoretical results for the interaction with a single cation show small interaction energy differences in the case of the alkali cations. This is comparable with the experimental results. When the influence of the zeolite lattice is introduced, here modeled by a cluster, adsorption energies of the same magnitude as the experimental ones, confirming an appropriate choice of our calculation model are found. However, the adsorption sequence is no longer in agreement with the experiment.

The experimental results are in agreement with the gravimetric measurements of Harlfinger et al., but in contradiction with the theoretical results presented here, predicting the highest adsorption enthalpy for 1-butene. A possible explanation, beside the fact that the theoretical calculations as well as the experi-

mental results are at limits of the techniques used, could be the effect of loss of entropy during the adsorption process, which is not included in the theoretical prediction. Several experimental studies showed the existence of a “so-called” compensation effect between the enthalpy and entropy of adsorption.^{17,25,26,45,46} For example, plotting the entropy of adsorption as a function of the adsorption enthalpy for a series of *n*-alkanes with different carbon number on a range of zeolites, yields a unique linear relationship.^{25,26,46} Although no sound theoretical explanation has been developed for this effect, one can easily understand that when a molecule has a strong interaction with an adsorbent, it will lose more freedom (entropy) than a loosely bound molecule. This demonstrates clearly that the relative importance of the entropy contribution in the Gibbs free energy is comparable to that of the enthalpy term.

trans-2-Butene, which has the lowest Henry constant, also has the highest (i.e., most negative) adsorption entropy, while isobutene, having the highest Henry constant, has the lowest adsorption entropy (Table 1), although the differences are quite small. Butane, which has a smaller adsorption enthalpy, has a lower adsorption entropy than the butene isomers (Table 1), which is in line with compensation effect consideration.

In our “static” approach, the molecule is put in the “region” where it is most probable that it will adsorb, in this case near the site II cation, and the geometry optimization will proceed till the most energetically favorable position (minimum of the potential energy) is found. In the real adsorbent–adsorbate system, a molecule might not reach the energetically most favorable configuration. This “entropy effect” can introduce a different behavior than expected theoretically, certainly taking into account the very small differences in adsorption enthalpy (see Table 1) found experimentally. Despite this, the theoretical results are in line with our chemical intuition, if we look, for example, to the electrical properties of the investigated molecules, as is discussed higher.

Conclusions

In this paper, the first ab-initio study on the adsorption of butene isomers in a faujasite-type zeolite is presented. We obtained interaction energies by quantum chemical calculations for four different butene isomers (isobutene, 1-butene, *cis*-2-butene, and *trans*-2-butene) with different cations in the gas phase and with a zeolite cluster containing Na⁺ as compensating cations.

The calculated interaction energies of the isomers with a given monovalent cation, which are the most important ones in this study since they can be compared with the experimental results, differ only slightly from each other in the gas phase; the range of values depends on the charge/radius ratio of the interacting cation. In the special case of sodium, which was also the cation present in the zeolite investigated experimentally, the difference between some isomers was less than a kcal/mol in the gas phase at the B3LYP/6-311+G** level.

While the strongest interaction with a cation (Na⁺) is found for isobutene in the gas phase, a different trend is obtained for adsorption in the NaY cluster, giving the highest energy for 1-butene. This change in adsorption trend can be explained by the fact that the zeolite framework gives 40% of its charge to the exchangeable cation, which influences the charge/radius ratio, thus the softness of the cation itself. The latter is in agreement with the results obtained for smaller cations with a higher charge. This result is also in agreement with the HSAB principle, since the hard Na⁺ cation interacts preferably with the hardest butene isomer, namely 1-butene.

Comparing the theoretical results for the interaction involving the zeolite with the experimental ones, it appears that the interaction energies have the right order of magnitude, indicating the right choice of calculation model. However, a different adsorption trend is found experimentally, showing very small differences in adsorption enthalpy between the different isomers. Experimentally determined Henry constants decrease in the order: isobutene > *cis*-2-butene > 1-butene > *trans*-2-butene, while the calculations predict the highest interaction energy for 1-butene.

The differences between the theoretical modeling for the theoretical enthalpies and the experimental data can be explained as follows: in the ab-initio calculations, the molecules are positioned in a region where they have a maximal interaction energy, while in the real system, the losses in entropical freedom might become too important in that region, for this the molecule will “sit” in a region where the optimal combination of enthalpy and entropy is obtained (Gibbs free energy).

However, some additional work should be performed in further investigations, such as refining the model, a dynamical study of the adsorption process, and the generation of experimental results with the bivalent cations.

Acknowledgment. F.T. thanks the Flemish Institute for support of Scientific-Technological Research in Industry (I.W.T.) for a postdoctoral fellowship. P.G. is indebted to the Free University of Brussels for a generous computer grant and to the F.W.O.-Flanders for continuous support. J.D. is grateful to the F.W.O.-Flanders, for a fellowship as postdoctoral researcher. This research was partly financed by the IUAP V-3 program of the Belgian Federal Government (Supramolecular Chemistry and Supramolecular Catalysis).

References and Notes

- (1) U.S. Pat. 6,022,398 (2000) to Korea Institute of Energy Research.
- (2) Jousse, F.; Leherste, L.; Vercauteren, D. P. *J. Mol. Catal. A* **1997**, *119*, 165.
- (3) Jousse, F.; Auerbach, S. M.; Vercauteren, D. P. *J. Phys. Chem. B* **1998**, *102*, 6507.
- (4) Tomlinson-Tschaufeser, P.; Freeman, C. M. *Catal. Lett.* **1999**, *60*, 77.
- (5) Schoofs, B.; Martens, J. A.; Jacobs, P. A.; Schoonheydt, R. A. *J. Catal.* **1999**, *183*, 355.
- (6) Schoofs, B.; Schuermans, J.; Schoonheydt, R. A. *Microporous Mesoporous Mater.* **2000**, *35*, 99.
- (7) Van Dun, J. J.; Dhaze, K.; Mortier, W. J.; Vaughan, D. E. *J. Phys. Chem. Solids* **1989**, *50*, 469.
- (8) Peirs, J.-C.; De Proft, F.; Baron, G.; Van Alsenoy, C.; Geerlings, P. *J. Chem. Soc., Chem. Commun.* **1997**, 531.
- (9) Tielens, F.; Langenaeker, W.; Ocakoglu, A. R.; Geerlings, P. *J. Comput. Chem.* **2000**, *21*, 909.
- (10) Tielens, F.; Geerlings, P. *J. Mol. Catal. A* **2001**, *166*, 175.
- (11) Tielens, F.; Geerlings, P. *Int. J. Quantum Chem.* **2001**, *84*, 58.
- (12) Tielens, F.; Geerlings, P. *Chem. Phys. Lett.* **2002**, *354*, 474.
- (13) Tielens, F.; Baron, G. V.; Geerlings, P. *Proceedings FOA7*; Nagasaki, Japan, 2002; p 393.
- (14) De Luca, G.; Arbouznikov, A.; Goursot, A.; Pullumbi, P. *J. Phys. Chem. B* **2001**, *105*, 4663.
- (15) Pearson, R. G. *J. Am. Chem. Soc.* **1963**, *85*, 3533.
- (16) Harlfinger, R.; Hoppach, D.; Quasick, U.; Quitzsch, K. *Zeolites* **1983**, *3*, 123.
- (17) Ruthven, D. M.; Kaul, B. K. *Adsorption* **1998**, *4*, 269.
- (18) Parr, R. G.; Yang, W. *Annu. Rev. Phys. Chem.* **1995**, *46*, 701.
- (19) Geerlings, P.; De Proft, F.; Langenaeker, W. In *Density Functional Methods: Applications in Chemistry and Material Science*; Springborg, M., Ed.; John Wiley: New York, 1997.
- (20) Geerlings, P.; De Proft, F.; Langenaeker, W. *Adv. Quantum Chem.* **1999**, *33*, 303.
- (21) Geerlings, P.; De Proft, F. *Int. J. Quantum Chem.* **2000**, *80*, 225.
- (22) Chermette, H. *J. Comput. Chem.* **1999**, *20*, 129.

- (23) Geerlings, P.; De Proft, F.; Langenaeker, W. *Chem. Rev.* **2003**, *103*, 1793.
- (24) Kärger, J.; Ruthven, D. M. *Diffusion in Zeolites and Other Microporous Solids*; John Wiley & Sons: New York, 1992.
- (25) Eder, F.; Stockenhuber, M.; Lercher, J. A. *J. Phys. Chem. B* **1997**, *101*, 5414.
- (26) Denayer, J. F. M.; Baron, G. V.; Jacobs, P. A.; Martens, J. A. *J. Phys. Chem. B* **1998**, *102*, 3077.
- (27) Katsanos, N. A.; Lycourghiotis, A.; Tsiatsios, A. *J. Chem. Soc., Faraday Trans.* **1978**, *74*, 575.
- (28) Atkinson, D.; Curthoys, G. *J. Chem. Educ.* **1979**, *12*, 802.
- (29) Sawyer, D. T.; Brookman, D. J. *Anal. Chem.* **1968**, *40*, 1847.
- (30) Okamura, J. P.; Sawyer, D. T. *Anal. Chem.* **1971**, *43*, 1730.
- (31) Koch, W.; Holthausen, M. C. A. *A Chemist's Guide to Density Functional Theory*; Wiley-VCH: Weinheim, 2000.
- (32) Becke, A. D. *J. Chem. Phys.* **1993**, *98*, 5648.
- (33) Lee, C.; Yang, W.; Parr, R. G. *Phys. Rev. B* **1988**, *37*, 785.
- (34) Stephens, P. J.; Delvin, F. J.; Chabrowski, C.; Firsch, M. J. *J. Phys. Chem.* **1994**, *98*, 11623.
- (35) Hehre, W. J.; Radom, L.; Schleyer, P. v. R.; Pople, J. A. *Ab Initio Molecular Orbital Theory*; Wiley: New York, 1986.
- (36) Frisch, M. J.; Trucks, G. W.; Schlegel, H. B.; Scuseria, G. E.; Robb, M. A.; Cheeseman, J. R.; Zakrzewski, V. G.; Montgomery, J. A.; Stratmann, R. E.; Burant, J. C.; Dapprich, S.; Millam, J. M.; Daniels, A. D.; Kucin, K. N.; Strain, M. C.; Farkas, O.; Tomasi, J.; Barone, V.; Cossi, M.; Cammi, R.; Mennucci, Pomelli, B.; C.; Adamo, C.; Clifford, S.; Ochteski, J.; Petersson, G. A.; Ayala, P. Y.; Cui, Q.; Morokuma, K.; Malick, D. R.; Rabuck, A. D.; Raghavchari, K.; Foresman, Cioslowski, J. B.; Ortiz, J.; J. V.; Stefanov, B. B.; Liu, G.; Liashenko, A.; Piskorz, P.; Komaromi, I.; Gomperts, R.; Martin, R. L.; Fox, D. J.; Keith, T.; Al-Laham, M. A.; Peng, C. Y.; Nanayakkara, A.; Gonzalez, C.; Challacombe, M.; Gill, P. M. W.; Johnson, B. G.; Chen, W.; Wong, M. W.; Andres, J. L.; Head-Gordon, M.; Replogle, E. S.; Pople, J. *Gaussian 98*, revision A.6; Gaussian Inc.: Pittsburgh, PA, 1998.
- (37) Van Alsenoy, C.; Peeters, A. *J. Mol. Struct. (THEOCHEM)* **1993**, *286*, 19.
- (38) Krishnamurty, S.; Pal, S.; Vetrivel, R. *Studies in Surface Science and Catalysis. (Recent Advances in Basic and Applied Aspects of Industrial Catalysis)* **1998**, *113*, 321.
- (39) van Duijneveldt, F. B.; van Duijneveldt-van de Rijdt, J. G. C. M.; van Lenthe, J. H. *Chem. Rev.* **1994**, *94*, 1873.
- (40) (a) Maginn, E. J.; Bell, A. T.; Theodorou, D. N. *Stud. Surf. Sci. Catal.* **1994**, *84*, 2099. (b) Snurr, R. Q.; Bell, A. T.; Theodorou, D. N. *J. Phys. Chem.* **1994**, *98*, 5111. (c) Smit, B.; Siepmann, J. I. *Science* **1994**, *264*, 1118. (d) Van Tassel, P. R.; Davis, H. T.; McCormick, A. V. *AIChE J.* **1994**, *40*, 925. (e) Maginn, E. J.; Bell, A. T.; Theodorou, D. N. *J. Phys. Chem.* **1995**, *99*, 2057. (f) Macedonia, M. D.; Maginn, E. J. *Mol. Phys.* **1999**, *96*, 1375.
- (41) Shannon, R. D. *Acta Crystallogr.* **1976**, *A32*, 751.
- (42) Buckingham, A. D. In *Intermolecular Interactions: From Diatomics to Biopolymers*; Pullman, B., Ed.; John Wiley & Sons: New York, 1978.
- (43) Maryott, A. A.; Buckley, F. *U.S. National Bureau of Standards Circular No. 537*, 1953.
- (44) Yang, W.; Parr, R. G. *Proc. Natl. Acad. Sci. U.S.A.* **1984**, *82*, 4049.
- (45) Atkinson, D.; Curthoys, G. *J. Chem. Soc., Faraday Trans. 1* **1981**, *77*, 897.
- (46) Bond, G. C.; Keane, M. A.; Kral, H.; Lercher, J. A. *Catal. Rev. - Sci. Eng.* **2000**, *42*, 323.